JOURNAL OF SOLID STATE CHEMISTRY 55, 353–361 (1984)

Defect Clusters in Wustite, $Fe_{1-x}O$

ALFRED B. ANDERSON,* ROBIN W. GRIMES,
AND ARTHUR H. HEUER

Department of Metallurgy and Materials Science, Case Western Reserve University, Cleveland, Ohio 44106

Received February 27, 1984; in revised form July 13, 1984

A quantum chemical approach based on predominantly covalent "normalized ion energies" has been developed for estimating structures and energies for defect clusters in quenched nonstoichiometric wustite ($Fe_{1-x}O$). Small defect clusters of zinc blende structure show special stability over other clusters considered. Of these, either a 13 : 5 or a 16 : 7 defect cluster (13 or 16 Fe^{3+} vacancies and 5 or 7 tetrahedral Fe^{3+} interstitials) have the proper structure and composition to account for the observed P′ and P″ phases in wustite.

Introduction

The lowest oxide of iron, wustite, exists as a stable phase only above 570°C. Wustite has the sodium chloride structure but at atmospheric pressure is always nonstoichiometric, and can be represented by $Fe_{1-x}O$, where x varies between 0.05 and 0.15. It has been known since the early work of Roth (*1*), and Koch and Cohen (*2*) that the nonstoichiometry is not accommodated by x iron vacancies, with $2x$ ferrous ions oxidized to the ferric state. Rather, the massive nonstoichiometry involves defect clusters in which some of the ferric ions occupy interstitial (tetrahedral) sites. It is now generally believed that these defect clusters involve the so-called 4 : 1 defect (*3–5*), in which a tetrahedral ferric interstitial cation is surrounded by four octahedral vacancies and four oxygen anions, as shown in Fig. 1. Structure models for the defect clusters based on X-ray (*2*), neutron (*6*), and electron diffraction data (*7, 8*) have been proposed with the constituent 4 : 1 defects sharing edges or corners, and there has also been a theoretical study (*9*) using ion–ion pairwise potentials, with polarization energies included.

From diffraction intensity ratios, it is possible to find the ratio of the number of octahedral vacancies (m) to the number of tetrahedral interstitials (n) (*6, 10*):

$$\rho = m/n$$

Gavarri *et al.* (*6*) determined that ρ was nearly constant and equal to 2.4 ± 0.5 over the whole range of wustite nonstoichiometry. If one assumes for present purposes that most vacancies in wustite are associated with defect clusters, themselves of constant size, then this ratio provides a measure of possible cluster size and composition.

Additional diffraction data (*7, 8, 11*) ex-

* Address correspondence to the Department of Chemistry, Case Western Reserve University, Cleveland, Ohio 44106.

0022-4596/84 $3.00

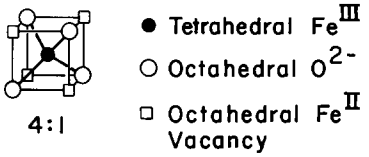

FIG. 1. The 4 : 1 cluster.

ists which can be interpreted in terms of two ordered defect phases, P′ and P″. P′ has been reported to have a disordered cubic incommensurate superstructure based on wustite with lattice parameter 2.6–2.7a, where a is the wustite lattice constant. P′ has been observed over the whole composition range. P″ forms only after slow cooling (*8*) or after subeutectoid aging (*7*); it is also based on wustite but has a commensurate cubic superstructure with lattice constant 5a. An explanation of the P′ and P″ ordering was given some time ago by Ijima (*12*); however, Lebreton and Hobbs (*8*) have shown that the evidence for the incommensurate character of P′ may be explained in terms of the small spatial extent of the ordered "domains" of defect clusters, i.e., the apparent incommensurate nature is an experimental artifact, P′ being simply a poorly ordered form of P″. The thermodynamic aspects of the formation of P′ and P″ have been discussed by Gavarri *et al.* (*13*).

Under all conditions of temperature and composition, the lattice parameter of wustite does not vary markedly from 0.432 nm. Even after the composition range for wustite is exceeded and magnetite (Fe_3O_4) becomes the stable phase, the equivalent lattice parameter of the anion sublattice only changes to 0.420 nm (*14*). Magnetite has the inverse spinel structure and can be represented as $(Fe^{3+})\{Fe^{2+}Fe^{3+}\}O_4^{2-}$, where the parentheses enclose tetrahedral ions and the braces enclose octahedral ions. The 4 : 1 cluster can be recognized as a structural component of the spinel lattice (Fig. 2), suggesting that the oxidation of wustite to magnetite may involve the formation and aggregation of defect clusters, although the basic cluster cannot have a spinel arrangement (*2*).

This paper describes a theoretical approach to determining and understanding the structures and stabilities of defect clusters in wustite. Comparisons will be made to the recent electron diffraction results for P′ and P″ wustite due to Lebreton and Hobbs (*8*), and the X-ray work of Koch and Cohen (*2*).

There are two approaches that can be adopted in defining the defect formation energy. We can begin with the idealized wustite lattice containing isolated cation vacancies, and then form the defect clusters, or the wustite lattice can be regarded as stoichiometric, with iron atoms then being removed to form the defects. For the latter process, the chemical reaction to form a 4 : 1 defect cluster in wustite is written as

$$9Fe^{2+}(o) \rightarrow Fe^{3+}(t) + 5Fe^{3+}(o) + 3Fe^{0} + 4V''_{Fe} \quad (1a)$$

where $Fe^{2+}(o)$ represents a ferrous ion on an octahedral site, $Fe^{3+}(o)$ a ferric ion on an octahedral site, $Fe^{3+}(t)$ a ferric ion on a tetrahedral site, Fe^{0} a neutral iron atom, and V''_{Fe} a vacant cation octahedral site.

Alternatively, using the Kroger–Vink (*15*) notation for (1a), we can write

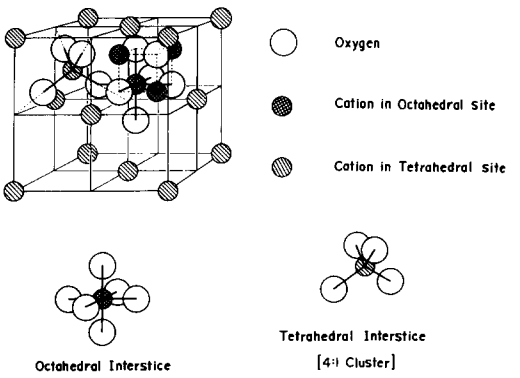

FIG. 2. The 4 : 1 cluster in the spinel lattice.

$$9Fe_{Fe}^{x} \rightarrow Fe_i^{\cdots} + 5Fe_{Fe}^{\cdot} + 3Fe + 4V_{Fe}'' \quad (1b)$$

where the subscripts refer to sites (i is an interstitial site), and the superscripts refer to formal charge relative to the usual valence of the stoichiometric phase, x representing normal charges, and $(\cdot)$ and $(')$ denoting positive and negative charges, respectively. In this notation, sites can only be added or removed in stoichiometric ratios, and all equations must be balanced for sites, charge, and mass. In the following, all equations will be written in both notations.

It is readily seen from Eqs. (1a) and (1b) that to form a 4 : 1 complex, five octahedral cations must be present in the ferric state, in addition to the ferric interstitial ion. For the general $m : n$ cluster of defects, one has

$$3(m-n)Fe^{2+}(o) \rightarrow n Fe^{3+}(t) + (2m-3n)Fe^{3+}(o) + (m-n)Fe^{0} + mV_{Fe}'' \quad (2a)$$

or

$$3(m-n)Fe_{Fe}^{x} \rightarrow n Fe_i^{\cdots} + (2m-3n)Fe_{Fe}^{\cdot} + (m-n)Fe + mV_{Fe}'' \quad (2b)$$

where the $2m - 3n$ holes are assumed to be delocalized in the vicinity of the cluster.

From the isolated vacancy clustering viewpoint, we may start with $m - n$ octahedral vacancies and two $(m - n)$ ferric ions and allow them to form an $m : n$ cluster corresponding to

$$2(m-n)Fe^{3+}(o) + (m-n)V_{Fe}'' \rightarrow n Fe^{3+}(t) + (2m-3n)Fe^{3+}(o) + mV_{Fe}'' \quad (3a)$$

or

$$2(m-n)Fe_{Fe}^{\cdot} + (m-n)V_{Fe}'' \rightarrow n Fe_i^{\cdots} + (2m-3n)Fe_{Fe}^{\cdot} + mV_{Fe}'' \quad (3b)$$

For any given cluster, either of the formulations corresponding to Eqs. (2) or (3) can be employed to calculate a cluster formation energy. However, the results of such calculations yield the energy of formation of a single cluster which incorporates $(m - n)$ preexisting ferrous ion vacancies (Eq. (3)) or equivalently was formed by the expulsion of $(m - n)$ iron atoms from the lattice (Eq. (2)). To permit comparison of clusters of different $(m - n)$ vacancies, we normalize the formation energy by the factor $(m - n)$. The difference between the values given by Eqs. (2) and (3) after normalization is a constant, equal to the energy of formation of an isolated vacancy by removing a single Fe cation. We have found it convenient to use the formulation of Eq. (3) within a quantum mechanical model for cluster energies, structures, compositions, and spacings.

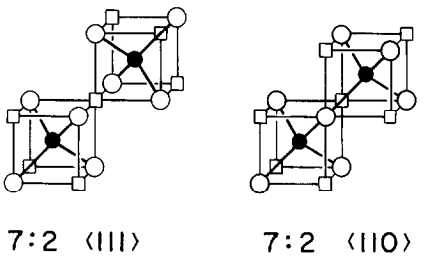

FIG. 3. The 7 : 2 ⟨110⟩ and ⟨111⟩ clusters.

Theoretical Model: Normalized Ion Energies

If the stability of Fe^{3+} relative to Fe^{2+} is the dominating driving force for defect cluster formation, then a naive crystal-field approach might be expected to apply. That is, the energy gained by cluster formation might be approximated by evaluating the d electron energy differences for the process given in Eqs. (2) and (3). However, such an emphasis on d electron energetics is incapable of distinguishing between, for example, the 7 : 2 ⟨110⟩ edge-sharing and 7 : 2 ⟨111⟩ corner-sharing clusters in Fig. 3. Consequently a traditional crystal field approach cannot be used as the sole input for quan-

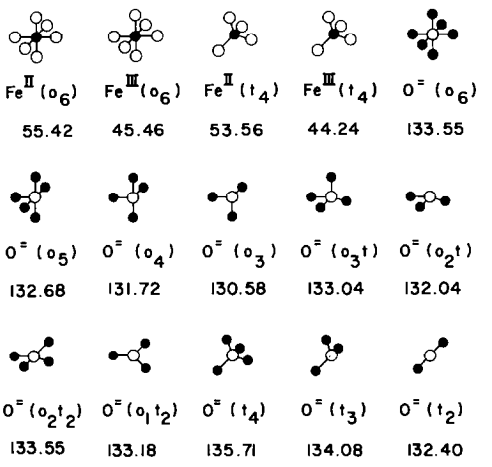

FIG. 4. Normalized ion structure and energies (−eV).

tum mechanical predictions of defect cluster structures and stabilities. A similar conclusion has been reached recently regarding the use of crystal-field data in attempting to predict whether a given spinel is normal or inverse (*16*).

As a simple *d* electron crystal-field approach is inappropriate, and pairwise potential approximations have convergence difficulties (*9*), another approach to the problem of predicting defect cluster structures and stabilities is necessary. One of the recently developed high-accuracy solid state calculational techniques might be used (*17*), especially for very small defect clusters and unit cells (not the case here), but we must of necessity start with a simpler model. Our quantum mechanical model assumes a rigid oxygen sublattice to avoid, as a starting approximation, the effects of lattice relaxations around the defect clusters, although such relaxations are known to affect results of other model approaches which use pairwise potentials (*9*).

Our model is a generalization of the *d* electron crystal-field approach to include the oxygen anion 2*s* and 2*p* orbital energies as well as the cation orbital energies. We call these energies normalized anion and cation energies. Our admittedly simple model omits long-range Madelung-like contributions to the defect cluster energies, but focuses instead on the covalent bond energy which includes polarization effects and short-range atom–atom repulsions. The adequacy of this type of theory is strongly supported by general conclusions in the literature concerning normal and inverse spinels (*16*), and a study of the wurtzite structure of BeO, where covalent aspects of the O anion energy were sufficient to produce Be–O–Be angles in agreement with tight-binding band calculations, a Madelung sum, and experiment (*18*).

ASED-MO Theory

In the calculations we use small cluster models to define cation and anion orbital energy levels and the total normalized ion energies, within the approximations of the one-electron atom superposition and electron delocalization molecular orbital (ASED-MO) theory (*19, 20*). It has recently been shown with regard to the optical properties of wustite, magnetite, and hematite that small cluster models yield energy levels which well-represent band energies for large clusters within the ASED-MO theory (*21*) (our parameters come from past studies of oxidized iron surfaces and wustite, hematite, and magnetite; see (*21*)). For example, the *d* energy levels in an FeO_6 model of hematite are at nearly the middle of the two *d* bands formed in an Fe_6O_{24} cluster where all six ferric cations are bulk-coordinated. The same is true for the O^{2-} 2*s* and 2*p* energy levels for OFe_6 and larger clusters.

Defect clusters in wustite contain octahedral and tetrahedral iron cations, and a total of 11 differently coordinated oxygen anions. The structures and normalized ion energies of these various components of the defect clusters, based on ASED-MO calculations, are shown in Fig. 4. Tetrahedral

Fe^{3+} and Fe^{2+} are 1.2 and 1.8 eV less stable than the corresponding octahedral cations. A comparable range of O^{2-} energies is found, with one three-coordinated O^{2-} being 5.1 eV less stable than tetrahedrally coordinated O^{2-}, which is the most stable species considered. The total normalized ion energies of various defect clusters are obtained by counting the number of anions and cations of each type which occur in and around each cluster, and summing their energies.

The ASED-MO theory includes a pairwise atom–atom repulsion energy, and a brief digression of this aspect of the theory is appropriate. The electronic charge density function of any molecule may be written as a sum of rigid free atom components and a delocalized bond-charge component. The binding energy is obtained by integrating the electrostatic force on a nucleus as atoms come together to form a bond. There are two components, a repulsive term due to rigid atom superposition, and an attractive term due to bond formation (*19a*). Their sum is exactly the binding energy. The repulsion energy is easily calculated, using charge densities from atomic wavefunctions, and is the pairwise energy mentioned above. Its Laplacian contains, to good accuracy, harmonic, cubic, and quartic force constants for molecules (*22*) and solids (*23*). Since the bond-charge density function is unknown, only an estimate of the attractive energy can be obtained. A one-electron orbital energy obtained by solving a Hamiltonian similar in form to the extended Hückel Hamiltonian is, for many purposes, a good approximation to the attractive binding energy due to electron-charge delocalization (*19b*). This readily applicable molecular orbital approach emphasizes the interaction energies which might be somewhat imprecisely called "covalent." Anion and cation valence orbital ionization potentials and anion valence orbital exponents are adjusted from the literature values to produce a reasonable charge transfer and bond length in diatomic FeO (*21*). To this extent, self-consistency and ionicity are included in our molecular orbital approximation to the electron delocalization energy. However, long-range ionic interactions are not included. Obviously we are using an approximate theory and model approach to the solid. The approximations and the model appear to go well together. The theory emphasizes orbital symmetries and overlaps within an ionic field due to the surrounding crystal, which is simply set equal to a constant first-order correction. The orbital interactions and bonding are known to be well-described by second-order perturbation theory terms which depend on orbital overlaps and energy differences (*24*).

The repulsion energy due to atom superposition, as described above, when combined with the extended Hückel-like orbital energy, allows calculation of bond lengths. For an octahedral Fe–O bond in the oxygen sublattice of wustite, the two-body repulsion energy is 0.0176 eV and for a tetrahedral Fe–O bond, it is 0.1286 eV.

Results: Cluster Structures and Energetics

As a first step, consider the clustering of two vacancies. In this case no interstitial Fe(t) forms and one has

$$2V''_{Fe} \rightarrow V''_{Fe}\text{–}V''_{Fe}, \qquad \Delta E = 0.19 \text{ eV}.$$

Two vacancies thus slightly repel one another. However, if a third vacancy is added adjacent to a Fe^{3+} ion, the latter can jump into a tetrahedral site, thereby forming a 4 : 1 cluster

$$V''_{Fe}\text{–}V''_{Fe} + V''_{Fe} \rightarrow 4:1 \text{ cluster}, \qquad \Delta E = -1.71 \text{ eV};$$

significant stabilization occurs, the 4 : 1 cluster forming with an overall stability of 1.52 eV. The greater stabilities of $O^{2-}(o_5)$ and $O^{2-}(o_3t)$ anions (see Fig. 4) more than

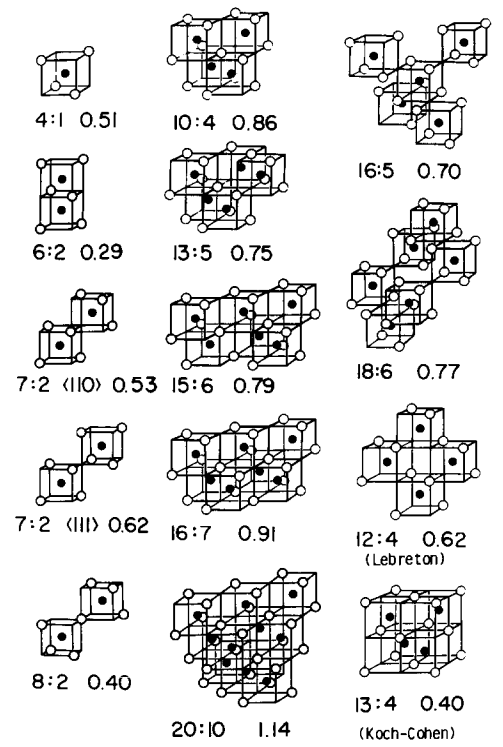

FIG. 5. Defect clusters and their binding energies per vacancy (−eV).

compensate for the destabilization of tetrahedral Fe cations relative to octahedral Fe cations in this cluster. The anion stabilities are a consequence of the complete octahedral coordination for $O^{2-}(o_6)$ and the short O–Fe(t) distance in $O^{2-}(o_3t)$; both cause covalent stabilization of O relative to the $O^{2-}(o_5)$ anions which occur within isolated vacancies.

It can readily be shown that some larger clusters produced by edge-, face-, or corner-sharing of 4:1 clusters are stable, and thus will lead to the formation of the P′ and P″ phases. However, only certain ordered defect clusters with a $m:n$ ratio of about 2.4 ± 0.5 form (*6*); Fig. 5 shows the structures and binding energy per vacancy for a number of the clusters studied which satisfy this condition. Other $m:n$ clusters of higher energy than those shown in Fig. 5 were studied but are not included here. Clusters with a zinc blende arrangement (tetrahedral Fe joined by tetrahedral O and comprising the middle column of Fig. 5) show the greatest stability, being more stable than the Lebreton 12:4 cluster (*8*) and the Koch–Cohen 13:4 cluster (*2*). (In fact the geometry of the Koch–Cohen cluster is incompatible with a cluster spacing of $2.5a$ because it is centered on an octahedral vacancy (*8*).) The zinc blende clusters owe their special stability to the large number of stable $O(t)$ anions they contain. Surprisingly, zinc blende-type defect clusters have not previously received much attention in the literature.

The stability of zinc blende-type clusters increases with cluster size and it was of interest to calculate the energy of an FeO cluster with the zinc blende structure, and to compare this with a similar calculation for rock salt FeO. We are gratified that the rock salt structure was the more stable (0.11 eV).

The model can also be used to find the energy gain when wustite with a stoichiometry of $Fe_{0.75}O$ transforms to the inverse spinel structure of magnetite. This energy is found to be 1.56 eV, which exceeds stabilities of all defect clusters examined.

P″, the most ordered phase of wustite, has defect clusters spaced $2.5a$ apart, as shown in Fig. 6, and occurs most readily in

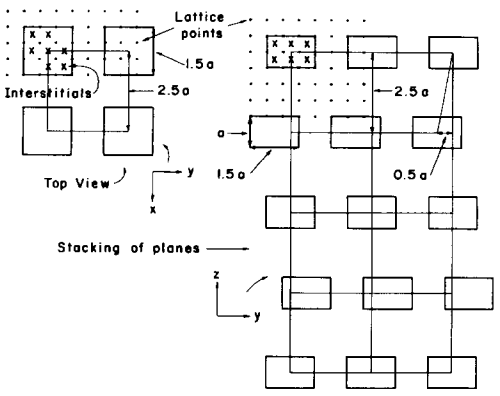

FIG. 6. Model for P″ phase composed of 16:7 defect clusters.

TABLE I

WARREN SHORT-RANGE ORDER PARAMETER, α_i, DETERMINED FOR A NUMBER OF CLUSTER TYPES

Vector	Experiment	13:4 Koch–Cohen	16:7 Zinc blende	13:5 Zinc blende	12:4 Lebreton	16:5 Spinel	8:3 Face-sharing
0 0 0	1	1	1	1	1	1	1
½ 0 0	0.57	0.37	0.32	0.28	0.25	0.20	0.21
1 0 0	0.35	0.19	0.16	0.04	0.09	−0.17	0.01
1 ½ ½	0.00	−0.01	−0.02	−0.05	−0.04	−0.02	−0.14
1 1 0	0.06	−0.08	−0.06	−0.07	−0.11	0.13	−0.19
½ ½ 0	0.11	−0.16	−0.16	−0.16	−0.11	−0.09	−0.14
1 1 1	−0.21	−0.16	−0.17	−0.17	−0.17	−0.17	−0.19
½ 1 ½	−0.26	−0.16	−0.21	−0.16	−0.17	−0.14	−0.19
½ ½ 0	−0.02	−0.16	−0.20	−0.19	−0.17	−0.09	−0.19
½ ½ 1	−0.37	−0.16	−0.21	−0.19	−0.17	−0.17	−0.19

wustites with composition between $Fe_{0.88}O$ and $Fe_{0.89}O$. This composition range permits a calculation of the net number of vacancies per defect complex, $m - n$. We assume that the region of wustite between the complexes is stoichiometric. In the volume occupied by a single defect (2.5*a*), a total of p iron cations must exist, of which x will be vacant for any composition $Fe_{1-x}O$, provided the vacancy distribution was homogeneous. This same number of net vacancies must be present in the defect complex, so that $px = (m - n)$ (see Eq. (3)). Since a unit cell of a rock salt structure FeO has four metal cations, we obtain

$$x = (m - n)/4(2.5)^3.$$

The $(m - n)$ values of 7, 8, and 9 thus correspond to stoichiometries $Fe_{0.888}O$, $Fe_{0.872}O$, and $Fe_{0.856}O$, respectively; or for a given stoichiometry, say, $Fe_{0.88}O$, we expect 7.5 net vacancies per defect. In fact, for a stoichiometry of $Fe_{0.88}O$, 7.5 net vacancies is a minimum number, as a perfectly ordered crystal of P″ is never obtained, and we thus focus on the 13:5 and 16:7 clusters. (Any imperfection in the ordering implies a larger number of net vacancies per defect.)

In order to show that the 16:7 and 13:5 models fit the existing X-ray diffraction data of Koch and Cohen (*2*), the Warren short-range order parameter (α_i) was calculated, for comparison with the experimental α_i. The α_i parameter is given by the equation

$$\alpha_i = \left(1 - \frac{P_{BA}^{UVW}}{X_A}\right)$$

where P_{BA}^{UVW} is the probability that the [UVW] vector from an A atom terminates on a B atom, and X_A is the random probability of a B atom being next to an A atom at the end of a vector [UVW]. In the present content, A is an occupied octahedral Fe site, and B is a vacant octahedral Fe site. We have also calculated α_i for a number of other defect clusters of interest; the data are collected in Table I.

It can be seen that the Koch–Cohen and 16:7 clusters give the best agreement with the experimental α_i data, with the 13:5 and 12:4 clusters being close behind. While the agreement with experiment for any of these models could be improved by slight displacements in the atom positions as Koch and Cohen attempted, such calculations would go beyond the spirit of this paper. It is important to note that the spinel cluster is eliminated from consideration by the large negative value of α_i for [100], while the 8:3 cluster found by Catlow and Fender (*9*) to have a large binding energy, gives consistently poor correlation (of course, the

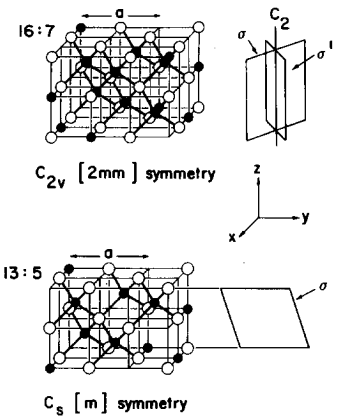

FIG. 7. The 16:7 and 13:5 clusters and their symmetry elements.

Koch–Cohen cluster is inconsistent with the TEM data of Lebreton and Hobbs (*8*)). The three defects remaining 16:7, 13:5, and Lebreton 12:4 all give more or less acceptable fits to the diffraction data, with the 16:7 having the greatest binding energy and the best fit to the Patterson (α_i) data, while the 12:4 has the lowest binding energy.

For these reasons, we favor the 16:7 and 13:5 clusters, which are shown in greater detail in Fig. 7. To decide between them will probably require either more refined calculations or further high-resolution electron microscopy studies.

In the P″ phase, clusters are aligned in a cubic array of $2.5a$ in one plane, but are offset by $0.5a$ in the third dimension (*8*). Both the 13:5 and 16:7 clusters allow such an arrangement; the 16:7 cluster was used to draw Fig. 6. On the ⟨100⟩ plane, alignment is perfect, except for the possibility that the clusters might be randomly rotated about the C axis. The orientation of the 16:7 clusters about the C axis in the different planes are unspecified in Fig. 6. Between planes, a 0.5 ⟨110⟩ shift is possible, giving rise to the zigzag seen by Lebreton (*8*).

Discussion and Summary

We have developed a model for defect clustering in quenched wustite using cation and anion energies. The method is based on the supposition that an energy may be defined for an ion in a solid and that this energy depends primarily on coordination. The normalized ion energy is determined using the one-electron atom superposition and electron delocalization molecular orbital (ASED-MO) theory. The normalized ion energies have added to them nearest neighbor pairwise repulsion energies that are a part of the ASED-MO theory. Using the established fixed oxygen anion sublattice for wustite, we have found zinc blende-type defect clusters are most favored because of the relative stability of the oxygen anions in this type of cluster. Of these, either a 13:5 or 16:7 cluster fits the compositional and structural data for the metastable P″ phase of wustite reasonably well. Either cluster will be surrounded by clouds of electron holes (octahedral ferric ions) which we suspect provides the cluster interactions responsible for defect cluster spacing and ordering.

We expect that such defect clusters will "evaporate" at elevated temperatures, dispersing isolated point defects throughout the wustite matrix because of the gain in configurational entropy. We have not taken this point into account in any of our calculations, but recognize that at any elevated temperatures, equilibrium will be maintained between the most stable defect clusters and the isolated point defects.

Finally, our model allows us to correctly deduce that magnetite is stable relative to $Fe_{0.75}O$ wustite, and that wustite is more stable in the rock salt than the zinc blende structure.

Acknowledgments

This research has been supported by the National Science Foundation through Grant DRM81-19425 to

the Materials Research Laboratory at Case Western Reserve University. We thank L. W. Hobbs for informative discussions.

References

1. W. L. Roth, *Acta Crystallogr.* **13,** 140 (1960).
2. F. Koch and J. B. Cohen, *Acta Crystallogr. Sect. B* **25,** 275 (1969).
3. P. Tarte, J. Prendhomme, F. Jeannot, and O. Evrard, *C.R. Acad. Sci. Fr. C* **269,** 1529 (1969).
4. A. K. Cheetham, B. E. F. Fender, and R. I. Taylor, *J. Phys. C.* **4,** 2160 (1971).
5. N. N. Greenwood and A. T. Howe, *J. Chem. Soc. Dalton* **1,** 110 (1972).
6. J. R. Gavarri, C. Carel, and D. Weigel, *J. Solid State Chem.* **29,** 81 (1979), and references therein.
7. B. Andersson and J. O. Sletnes, *Acta Crystallogr. Sect. A* **33,** 268 (1977).
8. C. Lebreton and L. W. Hobbs, *Radiat. Eff.* **74,** 227 (1983).
9. C. R. A. Catlow and B. E. F. Fender, *J. Phys. C* **8,** 3267 (1975).
10. E. Bauer and A. Pianelli, *Mater. Res. Bull.* **15,** 177 (1980); E. Bauer, A. Pianelli, A. Aubry, and F. Jeannot, *Mater. Res. Bull.* **15,** 323 (1980).
11. J. Manec, *J. Phys. (Ornay, Fr.)* **24,** 447 (1963).
12. S. Iima, "Diffraction Studies of Real Atoms and Real Crystals," pp. 217–218, Australian Academy of Science, Canberra (1974).
13. J. R. Gavarri, C. Carel, S. Jasienska, and J. Janowski, *Rev. Chim. Miner.* **18,** 608 (1981).
14. M. E. Fleet, *Acta Crystallogr. Sect. B* **37,** 917 (1981).
15. F. A. Kroger and V. J. Vink, *in* "Solid State Physics: Advances in Research and Applications" (F. Seitz and D. Turnbull, Eds.), Vol. 3, Academic Press, New York (1956).
16. J. K. Burdett, G. D. Price, and S. L. Price, *J. Amer. Chem. Soc.* **104,** 92 (1982).
17. M. T. Yin and M. L. Cohen, *Phys. Rev. B* **26,** 5668 (1982).
18. J. K. Burdett and T. R. McLarnan, *J. Amer. Chem. Soc.* **104,** 5229 (1982).
19. (a) A. B. Anderson, *J. Chem. Phys.* **60,** 2477 (1974); (b) **62,** 1187 (1975).
20. A. B. Anderson, R. W. Grimes, and A. H. Heuer, "Proceedings, 3rd International Conference on Transport in Non-Stoichiometric Compounds," Penn State Univ., June 10–16, 1984, Plenum Press, in press.
21. N. C. Debnath and A. B. Anderson, *J. Electrochem. Soc.* **129,** 2169 (1982).
22. A. B. Anderson and R. G. Parr, *J. Chem. Phys.* **53,** 3375 (1970); *Chem. Phys. Lett.* **10,** 293 (1971).
23. A. B. Anderson, *J. Chem. Phys.* **63,** 4430 (1975).
24. R. Hoffmann, *Acc. Chem. Res.* **4,** 1 (1971).